Asian Journal of Chemistry; Vol. 29, No. 11 (2017), 2453-2458

ASIAN JOURNAL OF CHEMISTRY

https://doi.org/10.14233/ajchem.2017.20746

Characterization of Cellulose Phthalate and Ionic Conductivity of Cellulose Phthalate-$LiClO_4$ Complexes

ARUUKHAN DASHKHUU KHASBAATAR[1,*], UNG SU CHOI[2] and BAYANJARGAL OCHIRKHUYAG[1]

[1]Department of Chemical and Biological Engineering, School of Engineering and Applied Sciences, National University of Mongolia, P.O. Box 46A/257, zip code 14201 Main building of NUM, University Street 1, Sukhbaatar District, Ulaanbaatar, Mongolia
[2]Center for Urban Energy System Research, Green City Technology Institute, Korea Institute of Science and Technology, 5, Hwarang-ro 14-gil, Seongbuk-Gu, Seoul 02792, Republic of Korea

*Corresponding author: E-mail: d_khasbaatar@seas.num.edu.mn

Received: 1 May 2017; *Accepted*: 2 August 2017; *Published online*: 29 September 2017; AJC-18570

In this article, ion-conducting solid polymer electrolytes based on cellulose phthalate (CP) with lithium perchlorate were prepared by the solution casting method. The host polymer cellulose phthalate was successfully synthesized and characterized by Fourier transform infrared analysis, HR X-Ray diffraction, scanning electron microscopy, thermogravimetric analyzer. The maximum degree of substitution of phthalic groups on anhydroglucose unit of cellulose (CPm) was 2.33. Ionic conductivities of CPm-$LiClO_4$ complexes were studied with various salt concentration and temperatures. The ionic conductivity was investigated using alternating current (AC) impedance spectroscopy. The highest ionic conductivity (2.54×10^{-5} S/cm) at room temperature was obtained for CPm-$LiClO_4$-4 when the ratio between degree of substitution (DS) of CPm and $LiClO_4$ is 2.33:2.0. Ionic conductivity of CPm complex was increased with the increase of temperature due to free volume theory. The trends of the ionic conductivity of CPm complexes were fitted to Arrhenius behaviour.

Keywords: Cellulose phthalate, Ionic Conductivity, Solid polymer electrolyte, HR X-Ray, Degree of substitution.

INTRODUCTION

Polymer electrolytes are considered attractive materials for the electrochemical community in the last decade due to their potential applications in electrically driven actuators [1], energy storages [2], sensors [3] and fuel cells [4]. The polymer electrolytes can be described in three folds including solid polymer electrolyte, gel polymer electrolytes and liquid polymer electrolyte [5]. In solid polymer electrolytes, the polymer electrolyte system is formed by introduction of salt into polymer matrix. The matrix acts as a solid solvent along with lithium salt and does not contain any organic liquids. The main advantages of solid polymer electrolyte are shape, geometry, mechanical strength and a capability for strong electrode-electrolyte contact [6].

One of the most amplifying methods for the development of polymer electrolyte materials is a polymer blending which has attracted much attention as an easy and inexpensive [7]. Polymer electrolytes are prepared by complexing polymers containing polar groups with metal salts and dissolving salts in polymer hosts. A polymer host owes its favorable physico-chemical properties mainly to the dominating the presence of polar groups with large sufficient electron donor power to form coordination with cations and a low hindrance to bond rotation. Some polymers, such as poly(vinylidene fluoride), poly(vinyl pyrrolidone), poly(vinyl alcohol), poly(vinyl chloride) polymers and carboxylmethyl cellulose [8], are widely studied as a host material to prepare polymer electrolytes for specific applications [9].

However, one major disadvantage of solid polymer electrolyte is their relatively low ionic conductivity at ambient temperature [5]. Ion transfer takes place generally through a coupling between the ions and polymer segmental motion. Thus, interchange characteristics such as association and dissociation for ions in the solid polymer electrolyte are fundamental in consideration of obtaining the high conductivities ($> 10^{-5}$ S/cm) necessary to be useful in applications [5,10].

Cellulose is a polysaccharide consisting of a linear chain of several hundred to over ten thousand β (1-4) linked anhydro-glucose units (AGU). It is not only biocompatible and modifiable, but also great potential for an outstanding industrial material. Electrical insulating property of cellulosic materials is excellent when dry due to containing a large number of traps and exhibiting structural deformations at certain transition temperatures [11]. The readily accessible hydroxyl groups of cellulose support attachments by other functional groups for novel types of materials.

The most known method of cellulose modification is esterification that can imply the substitution of free hydroxyl groups, yielding different cellulose derivatives and increase a number of applications. However, cellulose esters principally may suffer from hydrolysis and exhibit very low conductivity when not plasticized [12].

In this study, cellulose phthalate is modified for a host polymer to prepare solid polymer electrolyte. Phthalic anhydride was selected for esterification of cellulose due to good plasticizing effects, bifunctional and cheaply available [13]. Therefore, it reports preparation of cellulose phthalates with various degrees of substitution (DS) on anhydroglucose units (AGU) of cellulose. The synthesis and structure of cellulose phthalate was examined using Fourier transform infrared spectroscopy, high-resolution X-Ray diffraction and field-emission scanning electron microscopy. Thermal property was also examined by thermogravimetric analysis and differential scanning calorimeter. Ionic conductivity properties of CPm-$LiClO_4$ complexes with various salt concentration and temperatures were also reported with direct altering current impedance spectroscopic method.

EXPERIMENTAL

Cellulose, sodium hydroxide and hydrochloric acid were purchased from Sigma Co., Ltd. Phthalic anhydrate, dimethyl sulfoxide (DMSO), pyridine, dimethylacetamide and isopropyl alcohol were provided from Dae Jung Chemicals & Metals Co. Ltd. Korea. Lithium perchlorate ($LiClO_4$) is supplied from Strem Chemicals Co. Ltd. USA.

A Fourier transform infrared spectra (4000-450 cm^{-1}, KBr disc) was recorded on a GX FT-IR Perkin Elmer spectrometer. The cellulose phthalate was observed in a FE-SEM (Hitachi S4200) at 15.0 kV. The degree of substitution was measured using an auto-titrator (Metrohm 728, Switzerland). HR X-Ray diffraction (Scintag PAD X) was used to determine the crystalline of compound. The HR X-Ray source was Ni-filtered CuKα (60 kV-300 mA). Also, thermal property of cellulose phthalate was investigated using a DuPont 951 thermogravimetric analyzer (TGA). Thermogram curves were obtained under a nitrogen atmosphere at a flow rate of 4 mL/min and scanning rate of 10 ºC/min and heating rates of 10 ºC/min from 25 to 600 ºC.

Synthesis of cellulose phthalate: Cellulose powder (1 g), phthalic anhydride (2.7-11 g), DMSO (50 g) and pyridine (0-10 g) were transferred into a round flask with a condenser and reacted at 60-140 ºC in an oil bath for 3-24 h with stirring at 250 rpm. The sample was precipitated 500 mL isopropyl alcohol and washed three times with isopropyl alcohol and water. The sample was dried in freeze drier at -50 ºC for 24 h.

Degree of substitution (DS): The traditional saponification method was used to determine degree of substitution. A dried sample of cellulose phthalate (0.1 g) was added to Erlenmeyer flask with exactly 100 mL of 0.1 N NaOH solution. It was shaken for 24 h at 200 rpm at room temperature. The solution was back-titrated with a 0.1 N HCl solution. Ester content (EC) was calculated as:

$$EC\ (\%) = \frac{(V_{25} - V_{HCl})C_{NaOH}M_{pa}}{10M}$$

where V_{25} is the volume sampled from the solution, V_{HCl} is the volume of HCl used for back titration, M is the dry mass of cellulose phthalate, M_{pa} is the molecular weight of grafted phthalic residue and C_{NaOH} is the initial concentration of NaOH in the solution.

The degree of substitution (DS) was then calculated as:

$$DS = \frac{162EC}{100M_{pa} - EC(M_{pa} - 1)}$$

where 162 is the molecular weight of anhydroglucose [14]. The degree of substitution is shown in Table-1.

Film preparation: The polymer electrolytes of CPm-$LiClO_4$, which were prepared with cellulose phthalate with the highest degree of substitution (2.33) value and with various $LiClO_4$ molar concentrations such as CPm-$LiClO_4$-1 (2.33:0.5), CPm-$LiClO_4$-2 (2.33:1), CPm-$LiClO_4$-3 (2.33:1.5), CPm-$LiClO_4$-4 (2.33:2), CPm-$LiClO_4$-5 (2.33:2.33), CPm-$LiClO_4$-6 (2.33:2.66) were prepared by the solution casting method. Calculated amounts of $LiClO_4$ was dissolved in dimethyl acetamide and stirred for 1 h. Then, certain amount of CPm was measured and added to the solutions to make specific concentration of polymer solution and stirred for 3 h. After dissolving thoroughly, the solutions were poured onto petri-dishes. The transparent films were obtained after drying in vacuum oven at 60 ºC for 48 h. Thickness of the films was ranged about 95-287 μm.

AC Impedance spectroscopy: AC impedance spectroscopy was performed with an Impedance/Gain-Phase Analyzer (SI 1260; Schlumberger Technologies) and Electrochemical Interface (SI 1286; Schlumberger Technologies). The frequency range measured was from 100 MHz down to 0.1 Hz. The working electrode was a Cu24 mmφ-disk electrode (surface area, 4.523 cm^2).

RESULTS AND DISCUSSION

Modification and the degree of substitution: Cellulose phthalate was synthesized from cellulose, phthalic anhydride in DMSO and presence of catalyst pyridine (Fig. 1). The degree of substitution (DS) of cellulose phthalate were synthesized with various reaction conditions such as changing molar ratio between phthalic anhydride (PA) and anhydroglucose units (AGU) (PA/AGU), reaction temperature, time and catalyst (pyridine).

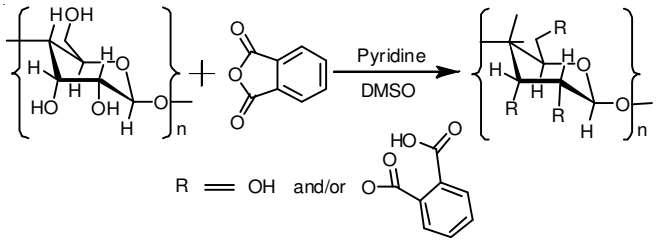

Fig. 1. Synthetic scheme of cellulose phthalate

It is shown in Table-1 that increasing molar ratio between PA/AGU from 2:1 to 12:1 could influence to increase of the degree of substitution (DS) values. Apparently, it was also seen that the increasing molar ratio provided more available phthalic anhydride in the medium. The degree of substitution (DS) value at the ratio 10:1 was slightly higher than the value at 12:1. However, no significant difference was observed the degree of substitution values between the ratios 10:1 and 12:1.

TABLE-1
CONDITION AND DEGREE OF SUBSTITUTION (DS) OF CELLULOSE PHTHALATE

Conditions						Cellulose phthalate	
DMSO (g)	Cellulose (g)	Pyridine (g)	Phthalic anhydride (molar ration PA/AGU)	Time (h)	Temperature (°C)	No.	Degree of substitution
50	1	5	2:1	6	100	1	0.22
50	1	5	3:1	6	100	2	0.5
50	1	5	6:1	6	100	3	2.07
50	1	5	8:1	6	100	4	2.12
50	1	5	10:1	6	100	5	2.33
50	1	5	12:1	6	100	6	2.3
50	1	10	10:1	6	60	7	0.44
50	1	10	10:1	6	80	8	1.13
50	1	10	10:1	3	120	9	2.05
50	1	10	10:1	3	140	10	2.03
50	1	10	10:1	3	100	11	1.43
50	1	10	10:1	4	100	12	1.72
50	1	10	10:1	5	100	13	2.01
50	1	10	10:1	12	100	14	2.15
50	1	10	10:1	24	100	15	2.19
50	1	–	10:1	6	100	16	0.29
50	1	–	10:1	12	100	17	0.32
50	1	–	10:1	24	100	18	0.47
50	1	5	10:1	6	100	19	0.85
50	1	7	10:1	6	100	20	1.46
50	1	13	10:1	6	100	21	2.29
50	1	15	10:1	6	100	22	2.31

The influence of temperature for cellulose phthalate was also studied. An effect of elevating temperature on phthalation reaction was necessary to enhance mobility of the reactant molecules and swellability of cellulose. Thus, DS values of the cellulose phthalate were increased by increasing reaction temperature from 60 to 100 ºC. However, when the reaction temperature rises over 100 ºC, the DS values were decreased due to degradation of cellulose that was probably caused by phthalation in high temperatures. In case of the increasing reaction time, sufficient time for phthalation was 6 h. No higher DS values were found by prolongation of the reaction time condition.

The effect of catalyst concentration and non-catalyst in medium was investigated as well. In the presence of catalyst, pyridine could act as a swelling agent [15] and an increase of DS value should be expected. The swelling might have impact to weaken the crystallinity, thus increasing the number of accessible reactive hydroxyl sites of cellulose. Moreover, the swelling could also cause mobility of hydrogen bonding and give anhydride more available to bond with hydroxyl groups. Addition of pyridine 5 g, 7 g and 13 g was allowed to increase DS values 0.85, 1.46 and 2.29, respectively due to reducing van der Waals forces and disrupting hydrogen bonding of networks within cellulose by pyridine. However, concentration of pyridine added over 10 did not affect either increasing or not considerably decreasing DS value. A preliminary loosening of the structure of cellulose did not increase phthalation.

It was found that the best DS value for phthalation of cellulose was obtained 2.33 that the reaction has been performed with 1 g of cellulose, 10:1 of PA/AGU, which is 9.1 g of phthalic anhydride (PA), 5 g of pyridine, at 100 ºC, for 6 h and in presence of 500 g of DMSO. Additionally, the cellulose phthalate with the maximum DS value was entitled CPm for further studies.

FT-IR study of cellulose phthalate: Fig. 2 shows the FT-IR spectra of cellulose (bold spectrum) and cellulose phthalate sample that were recorded in the 4000-700 cm^{-1} region. The bands at 3361, 2902, 1649, 1371, 1059 and 1052 cm^{-1} were associated with cellulose. A broad and intense band at 3361 cm^{-1} was assigned to free and hydrogen bonded OH stretching vibration of cellulose [16]. The peak at 2902 cm^{-1} was attributed to the asymmetric CH_2 stretching band. Water absorption of cellulose was observed at 1649 cm^{-1}. A band appeared at 1371 cm^{-1} was corresponded to OH bending. The absorption band at 1159 cm^{-1} was related to C-O stretching in acetyl group. C-O-C pyranose ring skeletal vibration was observed a strong peak at 1052 cm^{-1} [17].

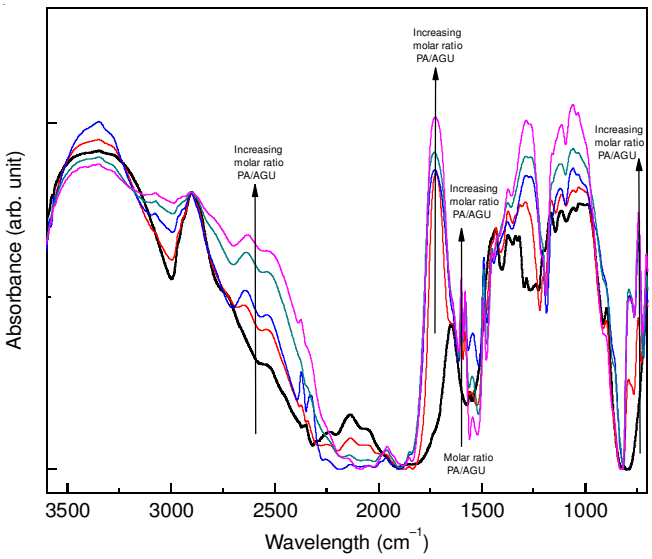

Fig. 2. FT-IR spectra for cellulose and increasing molar ratio phthalic anhydride (PA) and anhydroglucose units (AGU)

In spectra of cellulose phthalate as increasing PA/AGU is shown in Fig. 2. The intensity of the broad band in 2757-2321 cm^{-1} was increased due to the carboxylic acid dimer in cellulose phthalate. A very strong peak of carboxyl acid and carbonyl groups appeared at 1729 cm^{-1} which was attributed to C=O stretching bands which provided evidence of phthalation. This peak was also appeared due to anti-symmetric stretching of carboxylic in COOH groups which was observed at 1580 cm^{-1} [18,19]. A band at 1598 cm^{-1} was assigned to aromatic ring vibrations. The peak at 1163 cm^{-1} attributed to C-O stretching in the esters (O-(C=O)$CHCH_2$) on cellulose phthalate was overlapped at a peak of 1160 cm^{-1} that was exhibited in cellulose phthalate. The intensity of the band in the range 1300-1250 cm^{-1} increased. The band at 1292 cm^{-1} was corresponding to C-O symmetric stretching in ester. Also, the peak at 1290 cm^{-1} was assigned to stretching of carboxyl group. Increasing intensity of these bands could be enlightened that an ester and carboxylic acid were formed during the phthalation of cellulose. A band appeared at 741 cm^{-1} was assigned to wagging (out of plane bending) vibrations of carboxyl groups of cellulose phthalate. These peak alterations in the spectra of cellulose phthalate were indicated that phthalyl groups were introduce on the cellulose [20,21]. The intensities of carboxyl group bonds were increased due to incrementing DS values and the molar ratios. It should be mentioned that there were no sharp peak was observed in the region1904-1770 cm^{-1} in spectra of cellulose phthalate samples, which could be attributed to the absorption of anhydride carbonyl groups, thus, super-position of bands of phthalic anhydride stretching and cellulose phthalate has no phthalate anhydride [22].

HR X-ray of cellulose phthalate: HR X-ray diffraction (XRD) patterns obtained the cellulose phthalate electrolyte measured at room temperature including (a) cellulose, (b) 6:1 of PA/AGU and (c) 10:1 of PA/AGU as shown in Fig. 3.

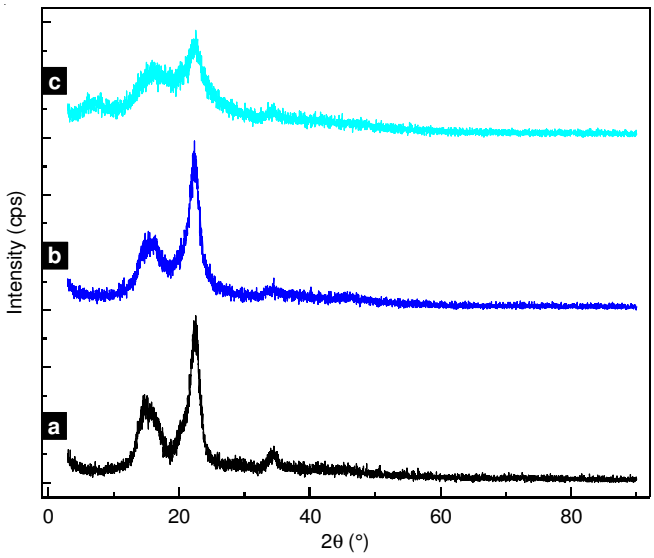

Fig. 3. HR X-ray diffraction of the cellulose and cellulose phthalate. (a) cellulose, (b) 6: 1 of PA/AGU and (c) 10: 1 of PA/AGU

In Fig. 3, three major crystallinity peaks at 2θ 15.2, 22.4 and 34.5 were observed. Decreasing tendency of the intensities of the peaks was observed as shown in Fig. 3(a-c). It means that amorphous phase of cellulose phthalate were increased as increasing DS value. Phthalation reaction was disrupting hydrogen bonding in the network of cellulose in order to introduce phthalic anhydride onto AGU of the cellulose. Thus, decreasing degree of order of arrangement hydrogen bonding between cellulose chains may have impact to destruct crystalline matrix and increase amorphous region on cellulose phthalate. Increasing amorphous region of cellulose phthalate could arouse molecular mobility of cellulose phthalate due to disordering structure and the relative of van der Waals bonding [23].

Thermal analysis of cellulose, cellulose phthalate and CPm-$LiClO_4$ and SEM of CPm-$LiClO_4$: The effect of phthalation on the thermal behavior of cellulose was also studied by TGA in the temperature range from room temperature to 600 °C at a rate of 10 °C/min under nitrogen flow. Fig. 4 shows the TGA thermograms of (i) cellulose and (ii) CPm and (iii) CPm-$LiClO_4$-4. A typical thermal degradation of cellulose was observed in Fig. 4(i). The cellulose was seen two main stages of weight loss behaviour. The first weight loss occurred at 90 ºC. This weight loss was caused by the volatilization of volatile matter and/or the evaporation of residual absorbed moisture. For cellulose, dehydration took place in a temperature range of 90-270 ºC, thermal degradation occurred rapidly at 270 ºC, and char was formed at 343 ºC. Most of the cellulose degraded at this temperature. In Fig. 4(ii), CPm was more stable than cellulose till the temperature increased to 140 °C. However, CPm was decomposed from 140 ºC to 348 ºC with 81 % weight loss, the decomposition temperature occurs at 294 ºC. These decreasing trends of decomposition temperature were implied that the thermal stability of cellulose phthalate was lower than that of the cellulose. In the case of CPm-$LiClO_4$-4 [Fig. 4 (iii)], the decomposition processes were analogously as rapid as CPm. Although, the decompositions were occurred slow when temperature reaches 270 ºC. It was caused from retardant properties of lithium salt.

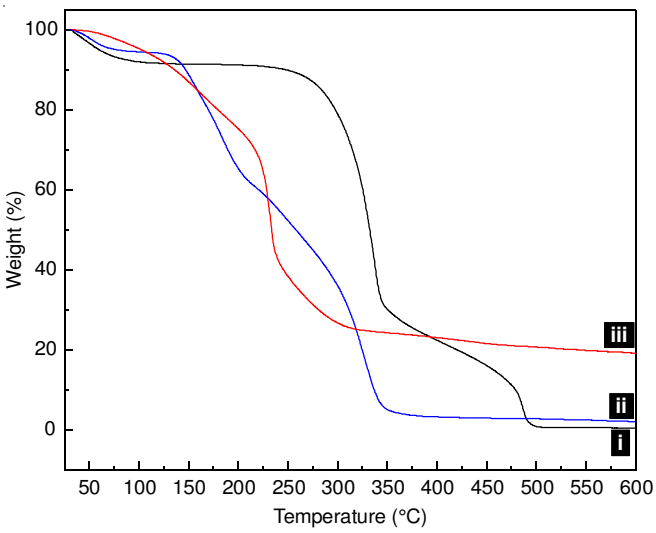

Fig. 4. TGA of cellulose and CP films (a) cellulose, (b) CPm and (c) CPm-$LiClO_4$-4

SEM images (Fig. 5) show the cross-sectional areas of CPm-$LiClO_4$ film. A uniform morphology was indicated in Fig. 5. No phase separation occurred for CPm-$LiClO_4$ electrolyte as well.

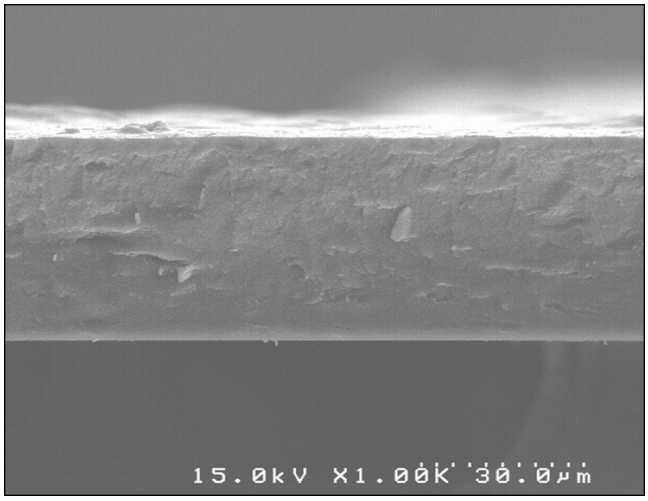

Fig. 5. SEM image of cross sectional area of the CPm-$LiClO_4$

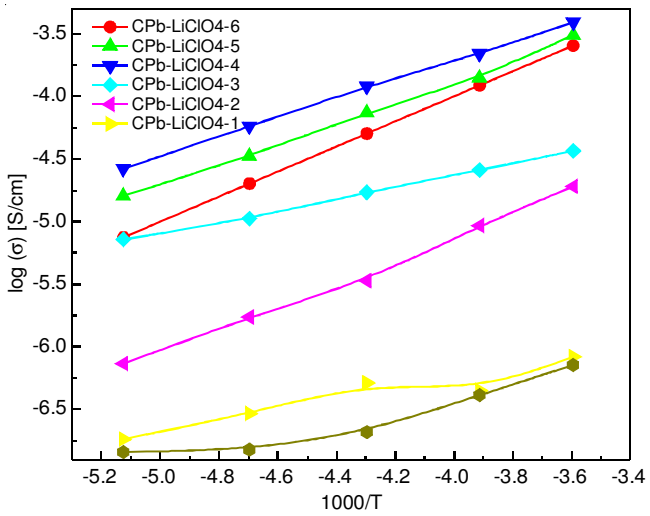

Fig. 6. Salt concentration and temperature dependence of ionic conductivity of CPm-$LiClO_4$polymer complexes

Conductivity study: The conductivity of a polymer electrolyte depends on the concentration of carriers and on their mobility. The values of ionic conductivity of CPm-$LiClO_4$ complexes with different concentration of $LiClO_4$ and increasing temperatures are shown in Table-2.The electrical conductivity of CPm was obtained 1.46×10^{-7} S/cm at room temperature due to the increase of intermolecular hydrogen bonding. When temperature increased, trend of the conductivity of CPm was raised to 7.16×10^{-7} S/cm at 373 K.

The highest ionic conductivity of CPm-$LiClO_4$ complexes at room temperature was obtained at 2.64×10^{-5} S/cm that corresponded to CPm-$LiClO_4$-4. The ionic conductivity was proportionally raised with the increase of the salt concentration of CPm-$LiClO_4$ complex from the sample CPm-$LiClO_4$-1 to CPm-$LiClO_4$-6 (Table-2) due to the increment of the amount of carrier ions introduced in CPm-$LiClO_4$ complexes. However, the salt concentration exceeded over 2.0, the ionic conductivity of CPm-$LiClO_4$ complex was decreased. It can be elucidated that increase of the salt concentration in CPm-$LiClO_4$ complex was amplified the number of carrier ions [24,25]. This leads to stronger ion-ion interactions between Li^+ carboxyl groups in cellulose phthalate, thereby, possibly inhibits ionic mobility and the polymer backbone's segmental motion. Thus, it caused a lowering of the conductivity. This feature was clearly seen in Table-2.

The Arrhenius plot (Fig. 6) was used to evaluate tendency of temperature dependence of ionic conductivity for cellulose phthalate complexes. The plot in Fig. 6 also shows that the conductivity increased with increase in temperature. Linearity of curves of the data points can be represented that this thermal reaction follows Arrhenius behaviour and first order reaction. Thus, when bond-breaking reaction takes place in CPm-$LiClO_4$ complex system, formation of dangling bonds in the system increases ion concentration. The ionic mobility is a function of the polymer segmental mobility [26]. Therefore, CPm-$LiClO_4$ complex can expand easily and produce free volume and local empty space, into which ionic carriers, solvated molecules, or polymer segments can move [27,28]. The resulting conductivity represented by the overall mobility of ion and polymer was determined by the free volume around the cellulose chains. On the other hand, at low temperature, ionic conductivity was decreased due to the shrinking free volume in the polymer and restricted ion motions.

Typical impedance plots for CPm-$LiClO_4$-4 complex with temperature range of 288-373 K and CPm at 288 K are shown in Fig. 7. The intercepts on the real axis gives the electrolyte bulk resistance. The conductivity of the polymer electrolyte was calculated from measured resistance of the known area and thickness of each polymer films. Semi-circle curve was observed in the high-frequency range of CPm. It meant that the conductivity of CPm corresponded to electron conduction. However, an absence of semi-circle portion that does not appear in the impedance response curves of CPm-$LiClO_4$-4 was indicated that the current carriers are mostly ions and therefore the total conductivity is mainly due to ion conduction [29]. The linearity in the high-frequency region is convincing evidence of the integrity of the film. On the other hand, increase of temperature could activate ionic mobility in the polymer complex thus impedance curve that was linear in room temperature was bent when temperature increases.

TABLE-2
CONDUCTIVITY OF CPm AND CPm-$LiClO_4$ COMPLEXES WITH INCREASING TEMPERATURES

Names	DS:$LiClO_4$	Conductivity (10^{-5} S cm^{-1})				
		298 K	313 K	333 K	353 K	373 K
CPm	2.33: 0	0.015	0.015	0.021	0.041	0.072
CPm-$LiClO_4$-1	2.33: 0.5	0.018	0.029	0.051	0.045	0.083
CPm-$LiClO_4$-2	2.33: 1	0.073	0.173	0.336	0.928	1.911
CPm-$LiClO_4$-3	2.33: 1.5	0.721	1.061	1.717	2.576	3.665
CPm-$LiClO_4$-4	2.33: 2	2.638	5.776	11.988	21.874	38.988
CPm-$LiClO_4$-5	2.33: 2.33	1.606	3.329	7.409	13.998	30.744
CPm-$LiClO_4$-6	2.33: 2.66	0.749	2.010	5.054	12.211	25.443

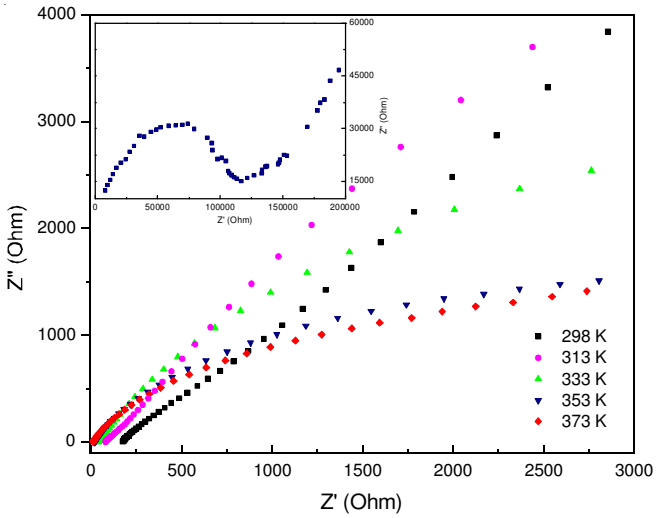

Fig. 7. Impedance diagram for CPm-$LiClO_4$-4 complex with increasing temperatures and the CPm (left top)

Conclusion

The cellulose phthalate was characterized using FT-IR, HR-XRD, and TGA. The peak at 1751 cm^{-1} corresponded to carboxylic and carbonyl groups was mainly implied to phthalation of cellulose and phthalic anhydride was successfully introduced on cellulose. There was no band in the range 1904-1770 cm^{-1} that would be attributed to super-position of bands of phthalic anhydride stretching. Phthalation reaction was disrupting hydrogen bonding in the network of cellulose in order to introduce phthalic anhydride to cellulose. Thus, HR-XRD studies were elucidated the occurrence amorphous region on cellulose phthalate. Thermogravimetric analyses revealed the thermal stability of cellulose phthalate and CP lithium complex. The highest ionic conductivity of CPm-$LiClO_4$-4 complex at room temperature (25 ºC) was observed at 2.64×10^{-5} S/cm. Ionic conductivity of CPm-$LiClO_4$ complexes was increased with the increase of temperature due to free volume theory. The trends of the ionic conductivity of CPm-$LiClO_4$ complexes were fitted to Arrhenius behaviour. Conducting polymer, CPm-$LiClO_4$, would be useful for energy storage and electroactive actuator applications.

ACKNOWLEDGEMENTS

This work has been done within the framework of the research project 17 (2015) supported by Asia Research Center, Mongolia and Korea Foundation for Advanced Studies, Korea and KIST.

REFERENCES

1. Q. Zhao, J.W.C. Dunlop, X. Qiu, F. Huang, Z. Zhang, J. Heyda, J. Dzubiella, M. Antonietti and J. Yuan, *Nat. Commun.*, **5**, 4293 (2014); https://doi.org/10.1038/ncomms5293.
2. G. Wang, L. Zhang and J. Zhang, *Chem. Soc. Rev.*, **41**, 797 (2012); https://doi.org/10.1039/C1CS15060J.
3. J. Migdalski, T. Blaz and A. Lewenstam, *Electrochim. Acta*, **133**, 316 (2014); https://doi.org/10.1016/j.electacta.2014.03.169.
4. Z. Cui, E. Drioli and Y.M. Lee, *Prog. Polym. Sci.*, **39**, 164 (2014); https://doi.org/10.1016/j.progpolymsci.2013.07.008.
5. A. Manuel Stephan and K.S. Nahm, *Polymer*, **47**, 5952 (2006); https://doi.org/10.1016/j.polymer.2006.05.069.
6. S. Rajendran, R.S. Babu and P. Sivakumar, *J. Power Sources*, **170**, 460 (2007); https://doi.org/10.1016/j.jpowsour.2007.04.041.
7. K. Kesavan, S. Rajendran and C.M. Mathew, *Polym. Sci. Ser. B*, **56**, 520 (2014); https://doi.org/10.1134/S1560090414040034.
8. M.I.H. Sohaimy and M.I.N. Isa, *Fibers Polym.*, **16**, 1031 (2015); https://doi.org/10.1007/s12221-015-1031-8.
9. C.V. Subba Rao, M. Ravi, V. Raja, P.B. Bhargav, A.K. Sharma and V.V.R. Narasimha Rao, *Iran. Polym. J.*, **21**, 531 (2012); https://doi.org/10.1007/s13726-012-0058-6.
10. V.L. Finkenstadt, *Appl. Microbiol. Biotechnol.*, **67**, 735 (2005); https://doi.org/10.1007/s00253-005-1931-4.
11. P.K. Khare, J.M. Keller, M.S. Gaur, R. Singh and S.C. Datt, *Polym. Int.*, **35**, 337 (1994); https://doi.org/10.1002/pi.1994.210350406.
12. M. Chelmecki, W.H. Meyer and G. Wegner, *J. Appl. Polym. Sci.*, **105**, 25 (2007); https://doi.org/10.1002/app.26108.
13. M. Rahman and C.S. Brazel, *Prog. Polym. Sci.*, **29**, 1223 (2004); https://doi.org/10.1016/j.progpolymsci.2004.10.001.
14. A.D. Khasbaatar, Y.J. Chun and U.S. Choi, *Polym. J.*, **40**, 302 (2008); https://doi.org/10.1295/polymj.PJ2007127.
15. A.N. Papadopoulos, *Holz Roh- Werkst.*, **64**, 245 (2006); https://doi.org/10.1007/s00107-006-0110-3.
16. C. Saikia, A. Hussain, A. Ramteke, H.K. Sharma, P. Deb and T.K. Maji, *Iran. Polym. J.*, **24**, 815 (2015); https://doi.org/10.1007/s13726-015-0370-z.
17. K. Bilba and A. Ouensanga, *J. Anal. Appl. Pyrolysis*, **38**, 61 (1996); https://doi.org/10.1016/S0165-2370(96)00952-7.
18. S.-B. Lee, Polymer Interfaces and Emulsions, Marcel Dekker, Inc, New York (1999).
19. T. Yoshimura, K. Matsuo and R. Fujioka, *J. Appl. Polym. Sci.*, **99**, 3251 (2006); https://doi.org/10.1002/app.22794.
20. R. Jayakumar, R. Balaji and S. Nanjundan, *Eur. Polym. J.*, **36**, 1659 (2000); https://doi.org/10.1016/S0014-3057(99)00244-X.
21. A.D. Khasbaatar, Y.G. Ko and U.S. Choi, *React. Funct. Polym.*, **67**, 312 (2007); https://doi.org/10.1016/j.reactfunctpolym.2007.01.003.
22. L.M. Matuana, J.J. Balatinecz, R.N.S. Sodhi and C.B. Park, *Wood Sci. Technol.*, **35**, 191 (2001); https://doi.org/10.1007/s002260100097.
23. J.R.E. Barker and C.R. Thomas, *J. Appl. Phys.*, **35**, 3203 (1964); https://doi.org/10.1063/1.1713200.
24. H.Y. Yang, G. Wu, H. Chen, F. Yuan, M. Wang and R.-J. Fu, *J. Appl. Polym. Sci.*, **101**, 461 (2006); https://doi.org/10.1002/app.23291.
25. S. Rajendran, P. Sivakumar and R.S. Babu, *J. Power Sources*, **164**, 815 (2007); https://doi.org/10.1016/j.jpowsour.2006.09.011.
26. Y.K. Siew, G. Sarkar, X. Hu, J. Hui, A. See and C.T. Chua, *J. Electrochem. Soc.*, **147**, 335 (2000); https://doi.org/10.1149/1.1393196.
27. M. Armand and J.-M. Tarascon, *Nature*, **451**, 652 (2008); https://doi.org/10.1038/451652a.
28. M.A. Ratner and D.F. Shriver, *Chem. Rev.*, **88**, 109 (1988); https://doi.org/10.1021/cr00083a006.
29. M.M.E. Jacob, S.R.S. Prabaharan and S. Radhakrishna, *Solid State Ion.*, **104**, 267 (1997); https://doi.org/10.1016/S0167-2738(97)00422-0.